CT NUMBER CHANGES WITHIN DEPTH IN CT AND CBCT IMAGES

BY

SYARIFAH NURFAJRINA BINTI SYED JUNIT

Dissertation submitted in partial fulfillment of the requirements for the degree of Bachelor of Health Science (Medical Radiation)

2015

CERTIFICATE

This is to certify that the dissertation entitled

CT Number Changes Within Depth in CT and CBCT Images

is the bona fide record of research work done by

SYARIFAH NURFAJRINA BINTI SYED JUNIT

during the period of February 2015

to June 2015

under our supervision.

Supervisor,

Mr. Mohd Fahmi bin Mohd Yusof,
Lecturer,
School of Health Sciences,
Universiti Sains Malaysia,
16150 Kubang Kerian,
Kelantan.
Date :

Co-supervisor,

Mr. Che Nazri bin Che Husin,
Senior radiographer,
School of Health Sciences,
Universiti Sains Malaysia,
16150 Kubang Kerian,
Kelantan.
Date :

ACKNOWLEDGEMENT

All praise to Allah, the *Most Gracious, Most Merciful* on whom we ultimately depend for sustenance and guidance. First, I would like to give my sincere appreciation to my supervisor, Mr. Mohd Fahmi bin Mohd Yusof for his brilliant idea, guidance, careful reading and constructive comments. I express my sincerest appreciation for his valuable time spent answering questions and correcting mistakes that I had made thus making me finally been able to shape this study to its final form.

I am also deeply indebted to my co-supervisor, Mr. Che Nazri bin Che Husin for his invaluable advice and supervision from the beginning of this study. I also would like to thanks School of Health Sciences, Universiti Sains Malaysia and Hospital Universiti Sains Malaysia for giving me opportunity to handle and letting me used the phantom and machines for this study. Many thanks also given to all staffs that might have help in any way to complete this study.

Nevertheless, I would like to dedicate this study to my parent for all the constant moral and financial supports. Last but not least, special thanks to all my classmates, friends and lecturers for continuous help and contribution in the successful completion of this study.

TABLE OF CONTENTS

List of Tables.

List of Figures.

List of Abbreviations.

CT	Computed Tomography
CBCT	Cone Beam Computed Tomography
3D	3-dimension
FOV	Field of view
HU	Hounsfield unit
ROI	Region of interest
PPMA	Polymethyl methacrylate
CTDI	Computed Tomography Dose Index
S/N	Serial Number
HUSM	Hospital Universiti Sains Malaysia
UFC	Ultra fast ceramic
kV	Kilovoltage
mAs	Milliampere per second
mA	Milliampere
mm	Millimetre
cm	Centimetre
2D	2-dimension
IEC	International Electrotechnical Commission
OS	Operating system
CAD/CAM	Computer-aided Design/ Computer-aided Manufacturing
DICOM	Digital Imaging and Communications in Medicine
CIRS	Computerized Imaging and Reference Systems

ABSTRACT

This study was carried out to determine the effect of increased depth to CT number on CT and CBCT images. In addition, this study was done to establish scanning method on CT and CBCT modalities in order to provide more precise dosimetry calculation involving CT and CBCT. An electron density phantom with tissue equivalent plugs was used in this study. The plug phantoms of various tissue equivalent materials were placed at different depths between the centre and peripheral of the phantom and scanned using CT and CBCT modalities. Images for both modalities were acquired and CT numbers at different depth in the phantom were analyzed. The results showed that on CT images, water equivalent plug phantom showed highest changes of CT number from peripheral position to central position with 146.4% and the lowest was air cavity with 0.55%. The results in CBCT images showed that muscle tissue equivalent plug phantom gave the highest change of CT number at increased depth with 6842.17% and the lowest difference was given by dense bone tissue equivalent plug phantom with 11.72%. A comparison of change in CT number between CT and CBCT showed that CBCT images having higher rate of change of CT number from peripheral position to central position compared to that in CT images. As conclusion, the CT number was found to be significantly increase as the depth increased. Thus, dosimetry measurement using CT number is suggested to be done at central position of phantom considering the contribution of x-ray scattering to the point of measurement. A calibration of CT number is required for dosimetry measurement at positions nearer to the surface of medium.

ABSTRAK

Kajian ini dijalankan untuk menentukan kesan peningkatan kedalaman terhadap nombor *CT* pada imej *CT* dan *CBCT*. Tambahan lagi, kajian ini juga dibuat untuk mewujudkan kaedah pengimbasan pada modaliti *CT* dan *CBCT* bagi menyediakan pengiraan dosimetri yang lebih tepat melibatkan *CT* dan *CBCT*. Satu fantom ketumpatan elektron dengan palam-palam bersamaan tisu telah digunakan dalam kajian ini. Palam-palam fantom yang terdiri daripada pelbagai bahan bersamaan tisu telah diletakkan di kedalaman yang berbeza di antara tengah dan periferal fantom dan diimbas menggunakan modaliti *CT* dan *CBCT*. Imej-imej untuk kedua-dua modaliti diperolehi dan nombor *CT* untuk kedalaman berbeza dalam fantom dianalisis. Hasil kajian yang didapati di imej *CT* menunjukkan palam fantom bersamaan air menunjukkan perbezaan nombor *CT* tertinggi dari kedudukan periferal ke kedudukan tengah dengan 146.4% dan yang terendah merupakan ruang udara dengan 0.55%. Hasil kajian untuk imej *CBCT* menunjukkan palam fantom bersamaan otot tisu memberi perubahan nombor *CT* tertinggi mengikut peningkatan kedalaman dengan 6842.17% dan perbezaan terendah diberi oleh palam fantom bersamaan tulang padat dengan 11.72%. Perbandingan perubahan nombor *CT* di antara *CT* dan *CBCT* menunjukkan imej *CBCT* mempunyai perubahan nombor *CT* tertinggi dari kedudukan periferal ke kedudukan tengah jika dibandingkan dengan imej *CT*. Sebagai konklusi, nombor *CT* didapati akan meningkat secara signifikan mengikut peningkatan kedalaman. Oleh itu, pengukuran dosimetri menggunakan nombor *CT* dicadangkan untuk dilakukan di kedudukan tengah fantom dengan mempertimbangkan sumbangan taburan dari sinar-X ke titik pengukuran. Kalibrasi nombor *CT* juga diperlukan untuk pengukuran dosimetri di kedudukan yang berdekatan dengan pemukaan media.

INTRODUCTION

1.1 Background of study.

Computed Tomography (CT) scanners are widely used in medical practice as it provides more diagnostic information than conventional X-ray. CT scan are preferable because it provides better image quality and has the ability to produce 3-dimentional (3D) images through cross sectional slices created by the scanner. The working principle of the currently used third generation CT scan is rotate-rotate principle where the X-ray tube rotates 360° throughout a doughnut shape structure that holds the tube in place. Opposing the X-ray tube is an array of image detectors that also rotate in conjunction with the x-ray tube in the rotating frame. The x-ray tube produces a fan beam of x-ray and detector array will read the signals that transmitted through the patient's body at each rotation. An image in form of slice of image is created along this process.

Although CT scan has shown an incredible usage in medical, there are limitation for it especially in dentistry application due to dose consideration and cost ineffectiveness. Thus, a cone beam computed tomography technique was introduced known as Cone Beam Computed Tomography (CBCT). It is a specifically designed scanner which is dedicated to the imaging of the maxillofacial region. The working principle of CBCT is slightly different to the CT scanner where the x-ray beam are in cone-shaped thus the larger field of view (FOV) creates slices of image with only one rotational sequence of the gantry (Scarfe & Farman, 2008). CBCT provide substantial dose reduction without loss of diagnostic information by using 180° tube rotation instead of 360° and this is possible due to larger FOV. (Lofthag-Hansen S. , 2010)

However, despite the usage of CBCT in dentistry, there are limitations of image quality from the CBCT scan which occur due to large FOV related to noise and contrast resolution that are cause by lots of scatter radiation involved (Scarfe & Farman, 2008). In order to differentiate each type of tissue on CBCT images, CT number is used with certain range of value representing certain types of tissue material thus helping in making contrast between the adjacent images are difficult to be evaluated by naked eyes. As well as in CT images, these CT numbers also give the same function with addition it is used in quality control to determining the dose uniformity in CT images.

CT number or Hounsfield Unit (HU) is the value of calculated x-ray attenuation coefficient of each voxel and becomes the value of the corresponding pixel in the digital CT image. By definition, the CT number of water is 0 and for air is -1000. CT number is very much dependent on tube voltage, filtration, electron densities or object thickness (attenuation coefficient) (Tsukihara, Noto, Hayakawa, & Saito, 2013). CT images quality can be determined by CT number uniformity over the image area where the value of CT number of each pixel should be the same with acceptance difference of < 8 HU. The CT number is given by the formula ;

$$\text{CT number} = \frac{\mu Material - \mu Water}{\mu Water} \times 1000 \qquad (1.1)$$

In every CT or CBCT images, reduction of CT number at the peripheral part of the image to the central part due to the attenuation of medium which increases significantly with depth. Basically, the peripheral part of the image should be receiving more radiation doses than the central part because during scanning due to less contribution of scattering by the surrounding medium, and higher proportion of primary beam. The outer part received mainly the primary beam as compared to the

central part. Thus, with beam hardening correction which are made to correct beam hardening artefact that are present in almost every CT or CBCT images due to the attenuation of high density material, this non-uniformities can be reduced.

However, on CBCT images, the distortion and reduction of CT numbers were expected to be more critical than on CT images. This is due to its working principle where most CBCT machine was scanned at 180° beam rotation (Jaju, Jain, Singh, & Gupta, 2013). Although cone-shaped beam is used which to cover most of the volume, the inner part (the detector side) still does not receive enough radiation due to the distance and attenuation of the medium that is closer to the x-ray source resulting in low CT number value at the inner part. Meanwhile, the CT number distortion and reduction from CT images only expected to be at the central part of the scanning object. This shows the contradiction between CT number distortion on CT images and CBCT images.

1.2 Aim.

The aim of the study is to determine the changes of CT number with depth in CT and CBCT images.

1.3 Objectives

The specific objectives of this study are:

1. To determine CT number at increased depth of density phantom.
2. To determine the effect of depth on CT number of CT and CBCT images.
3. To establish the scanning method for CT and CBCT modalities.

LITERATURE REVIEW

According to Mutic et al (2003), ideally, a CT scan of a uniform phantom would have uniform CT numbers throughout the image. However, this does not hold true as the CT numbers are usually not uniform due to random and systematic components. Noise is the random component of non-uniformity while the systematic component is due equipment design, beam hardening or image reconstruction software. In order to prove this non-uniformity, a field uniformity test can be done by scanning a uniform phantom then drawing fixed ROIs area throughout the phantom thus producing samples of mean CT numbers.

Based on the study done by Goldman (2007), the CT number non-uniformities occur due to beam hardening artefacts that are actually present in almost all CT images. The imperfect beam hardening correction used during image reconstruction results in the appearance of the artefact on CT images. These artefacts appear as non-uniformities in CT numbers where the values are lower at the centre of a uniform phantom and higher at the peripheral part. The difference are usually quite low (≤ 5 HU) unless narrow window level was used to view the image. The large CT number variation can also arise when the radiation passes through thick regions of bone or contrast medium which result in the clear appearance of beam hardening artefact.

Apart from that, some artefact are said to be more pronounced in CBCT counterpart than in CT images because of different processes involved in image acquisition procedure. Artefact related to CBCT images can be divided into three main categories which are physics-based, patient-based and scanner based artefact. Physics-based artefact comes from the physical processes which are involved in

data acquisition such as noise that happen due to low contrast resolution used in CBCT modalities and scatter radiation. Patient-based artefacts are due to factors related to patient's function or form for example metal streaking or motion artefact. Lastly, the scanner-based results from scanner functional defects as ring artefact which are rare in CBCT images (Jaju, Jain, Singh & Gupta, 2013).

In addition, a study done by Kiarudi, Eghbal, Safi, Aghdasi and Fazlyab (2015), stated that CBCT differs from CT in a few fundamental ways which make it more suitable for dental imaging although it was originated from conventional medical CT mechanism. CBCT has cone-shaped x-ray beam that captures a cylindrical or spherical volume of data that is called field of view (FOV). A 3D volume of data is acquired by one sweeping motion of the scanner in which the scanner and the detector is rotating oppositely in 180° to 360° around patient's head. During the exposure, planar projection images are obtained from FOV in an arc of at least 180°. This way, the CBCT machine can produce precise, essentially accurate and immediate 3D radiographic images.

Based on the study by Goldman (2007), the standard dosimetry phantoms that are being used are the cylindrical acrylic phantoms. This phantom has holes for dosimeter insertion at various locations. There are 2 sizes of phantom used for the CT dosimetry study which are head phantom in 16 cm diameter and body phantom in 32 cm diameter. This phantom is made up of polymethyl methacrylate (PPMA) with density of 1.19 g/cm^3 (near to water density which is 1.00 g/cm^3). In general, the CTDI measurement at different location and depth will be different. The CTDI at the centre of the head phantom is nearly the same as that periphery, where the centre CTDI would appear to be more than half of the peripheral CTDI.

MATERIALS AND METHODS

3.1 Materials.

3.1.1 Siemens SOMATOM Definition AS CT scanner.

In this study, the model of CT scanner used is the Siemens SOMATOM Definiton AS 128 slice (S/N 64280). This Siemens SOMATOM Definiton AS (Figure 3.1.1) is a third generation CT scanner that was installed on May 2009 in Department of Emergency of Hospital Universiti Sains Malaysia (Hospital USM). It constitute two x-ray source that works simultaneously and thus capable of working in fast and effective environment that requires speedy diagnosis such as Accident and Emergency Department. It has 595 mm of focus to isocentre distance and 1058 mm focus to detector distance.

In detection system, this machine uses solid state detector with Siemens UFC detector material. In order to fulfill the needs to obtain 128 slices, 64 detectors was installed along the z-axis as well as 736 of detector elements per row. The power rating for this CT scanner is 100 kV with 4 different kV setting which is 80 kV,100 kV,120 kV AND 140 kV with 20-800 mA range and 1mA of step size. Apart from common diagnosis examination, this machine also provides advanced examination in cardiology, neurology and oncology.

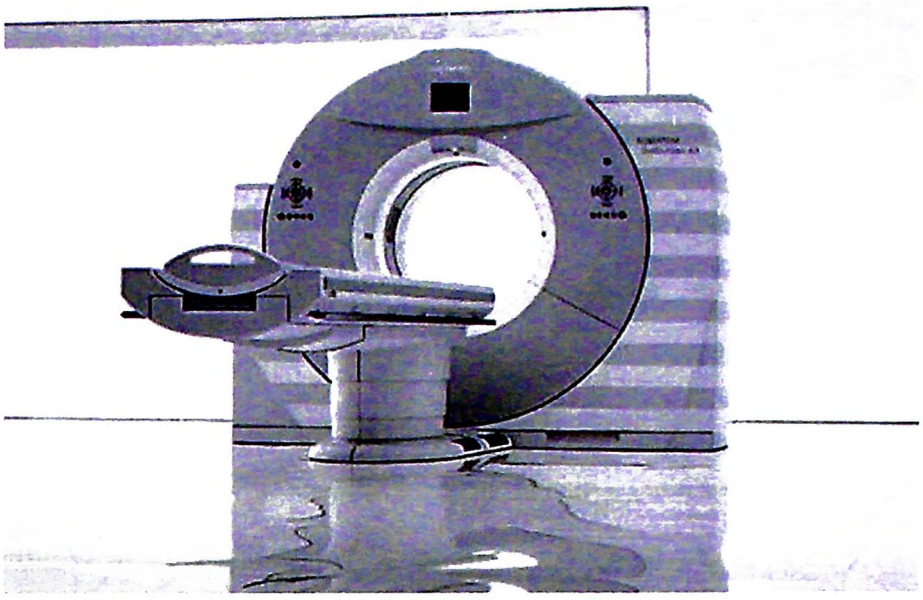

Figure 3.1: Siemens SOMATOM Definition AS CT scanner.

3.1.2 Syngo software for CT scanner.

Syngo.via software is accompanied along the Siemens SOMATOM Definition AS CT scanner which is used to read and translate the 3D images as well as for advanced visualization. This software provides a comprehensive suite for 3D reading applications. Syngo.via software also compliments a few of automated pre-processing routine steps and prior examinations are pre-fetched automatically. This software is user friendly where it helps students or first timer user to be able to use the software with ease. Thus, it can increase efficiency, quality, utilization and ROI. Syngo.via also has WebViewer feature which provide easy access for mobile devices therefore making it possible to view images and findings anywhere with software installation.

3.1.3 Planmeca ProMax 3D Cone Beam Computed Tomography machine.

The CBCT machine was used to acquire CBCT images for CT number determination. In HUSM, the only available dental CBCT imaging modality is the Planmeca ProMax 3D scanner. This machine provides 3D imaging as well as 2D panoramic and cephalometric imaging. For 3D mode, the tube voltage ranges between 60 kV and 80 kV, with anode current between 1 and 10 mA , 0.96 mm slice thickness and the scan time is about 17 seconds. The FOV size being used was 8 cm x 8 cm. The generator is resonant-mode with the standard IEC 60601-2-7:1998 with mounted x-ray tube which is Toshiba D-054SB-P. The focal spot size is 0.5 mm x 0.5 mm and the minimum total filtration is 2.5 mm Aluminium. This machine uses flat panel detector and has advanced large view volume stitching program that introduces low dose, large volume imaging based on selection of view up to 3 horizontal volumes and two vertical volumes (Planmeca, 2015)

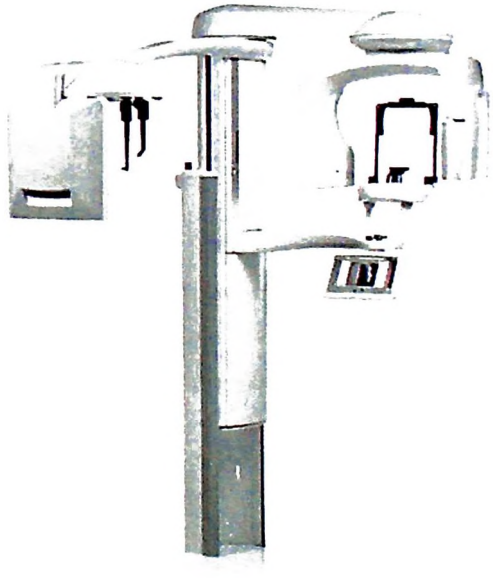

Figure 3.2 : Planmeca ProMax 3D machine.

3.1.4 Planmeca Romexis Viewer software.

The Planmeca Romexis Viewer software (Figure 3.1.4) was used to display and analyze CBCT images and to obtain CT number value for specific ROI drawn. This software comes together with the Planmeca ProMax 3D machine and it compatible for Apple Mac OS X and Microsoft Windows operating systems. It also support most versatile range of 2D and 3D imaging modalities. This software also easy to use for all images from X-ray to Computer-aided Design/ Computer-aided Manufacturing (CAD/CAM). Planmeca Romexis also able to import and export 2D and 3D images in standard format for example DICOM format. (Planmeca, 2015)

Figure 3.3: Planmeca Romexis Viewer software interface for CBCT image view and analysis.

3.1.5 CIRS Electron Density Phantom.

The CIRS Electron Density Phantom model 062M (Figure 3.4) was used as well as most of the tissue plugs that comes with it. All of the tissue plugs used are tissue equivalent materials and removable tissue plugs that makes every study done a lot convenient. Most of the tissue plug are in pair except for the certain optional plugs. Tissue plugs used in this study are solid dense bone, solid trabecular bone, liver, muscle, breast, adipose, water, lung inhale and lung exhale. This phantom is a electron density body phantom that consist of removable electron density head phantom. This phantom is made up of water and tissue equivalent epoxy resins. The whole phantom (body phantom) with specified tissue plugs were used in CT data collection while the head phantom with specified tissue plugs were used in CBCT data collection.

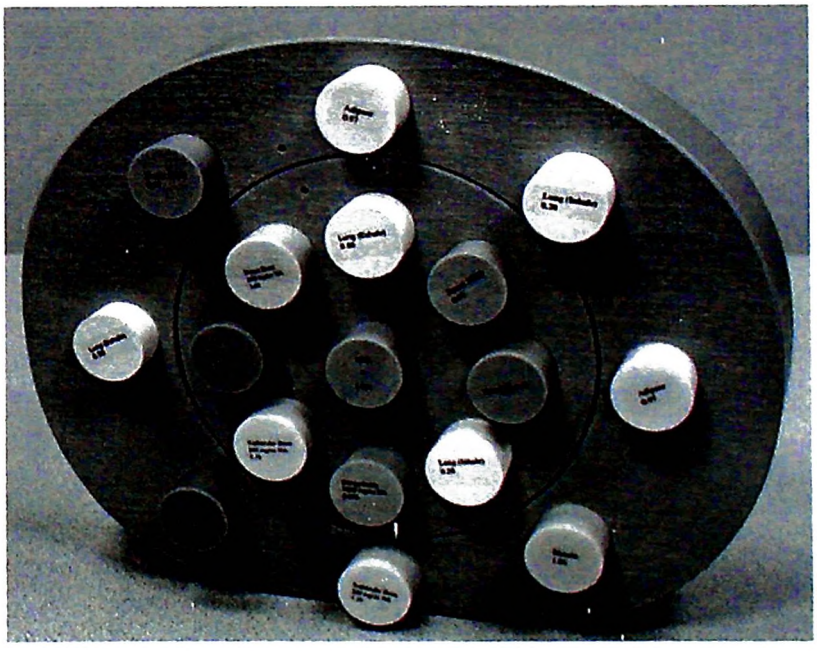

Figure 3.4 : CIRS Electron Density Head and Body Phantom with tissue plugs.

Table 3.1: CIRS Electron Density Phantom mass density and electron density (CIRS Inc, 2015)

Part number	Description	Physical density (g/cm^2)	Electron density x 10^{23} electrons/cc
062MA-01	Electron Density Head Insert	1.029	3.333
062MA-02	Electron Density Body without Head Insert	1.029	3.333
062A-04	Lung (Inhale) Equivalent Electron Density Plug	0.200	0.634
062A-05	Lung (Exhale) Equivalent Electron Density Plug	0.500	1.632
062A-06	Breast (50% Gland / 50% Adipose) Equivalent Electron Density Plug	0.990	3.261
062A-08	Solid Trabecular Bone (200mg/cc HA) Equivalent Electron Density Plug	1.160	3.730
062A-09	Liver Equivalent Electron Density Plug	1.070	3.516
062A-10	Muscle Equivalent Electron Density Plug	1.060	3.483
062A-11	Adipose Equivalent Electron Density Plug	0.960	3.171
062A-15	Solid Dense Bone (800 mg/cc) Equivalent Electron Density Plug	1.530	4.862
062MA-16	Water Equivalent Insert	1.000	3.333

3.2 Methods.

3.2.1 CT scanner.

The electron density phantom (head and body) with 9 tissue plug and air are irradiated with the same parameter used. The exposure factors used were 120 kVp and 250 mAs with 1.0 mm slice thickness and slices up to 15 slices for each irradiation. CAREdose was not applied for this study and the protocol used for the scan was the routine abdomen protocol. Each of the tissue equivalent material were irradiated at 3 different position (position X, Y and Z) within the density phantom as shown in Figure 3.2.1. Topogram (positioning scan) were done to make sure the phantoms are correctly placed on the couch. Due to limited number of tissue equivalent density plugs available, each type of material were irradiated twice. For the first irradiation, the tissue equivalent density plugs were placed at position X and position Y as shown in Figure 3.5. Then, for the next irradiation the tissue plugs were placed at position Y and position Z of the density phantom to acquire three different positions (Figure 3.5) within the phantom. The same positions was applied to all of the materials.

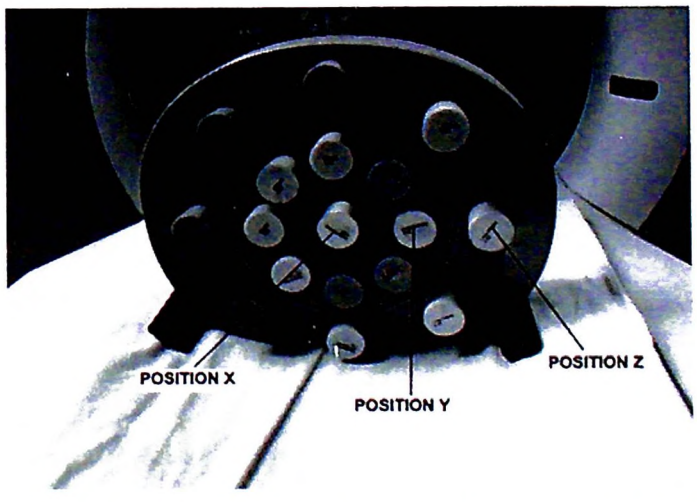

Figure 3.5: Phantom positioning and tissue plugs position.

After image reconstructions were carried out, the image was viewed in Syngo software and the CT number acquisition phase were preceded. The ROI's were carefully drawn onto each of the image slices. The ROI's were drawn at the centre of the tissue plug image and the circular areas used were measured to have almost the same value (0.61 cm^2) for all of the material. Then, the CT number were read and tabulated. The CT number data was afterwards being calculated to measure the percentage difference of the CT number between the depths for each of the materials used using formula as shown.

$$\text{Percentage Difference} = \frac{CT_c - CT_p}{CT_c} \times 100\% \qquad (3.1)$$

with CT_c and CT_p is the CT number measured at centre and peripheral of electron density phantom respectively.

3.2.2 CBCT scanner.

For this machine, only the head part of the electron density phantom was used due to size limitation and to simulate the head size of human. Thus, only the materials that are within the maxillofacial part were chosen and irradiated. The tissue equivalent materials that used were dense bone, trabecular bone, muscle, adipose tissue, water and air. Two tissue plug of each material were placed at the centre (position X) and outer part (position Y) of the head density phantom. Each of the material was irradiated and all of the material used same technical parameters which are 90 kVp and 10 mA for 12 seconds with slice thickness 0.96 cm.

The phantom was placed on the head stand of the machine (Figure 3.6). The head density phantom underwent positioning scan to make sure the phantom were

placed correctly. Then, the phantoms are irradiated with fixed parameter for all 6 materials. Images are obtained after reconstruction and data was acquired using the Planmeca Romexis Viewer software. ROI's were drawn onto each of the image slices with circular area 90.24 mm^2 applied for all of the ROI's. Then, CT number were read and tabulated. The CT number data was afterwards being calculated to measure the percentage difference of the CT number between the depths for each of the materials used using the same formula used for CT images.

Figure 3.6 : Head part of the electron density body phantom positioned on the head stand of CBCT machine.

RESULTS

4.1 Percentage discrepancy of CT number at various density tissue equivalent materials.

4.1.1 CT number at different depths on CBCT images

The graph of CT number against depth from surface of electron density phantom for various tissue equivalent plug phantoms on CBCT imaging were illustrated in Figure 4.1 until 4.6. Interpolation lines were drawn between the points of measurement to determine the rate of change of CT numbers at increased depth.

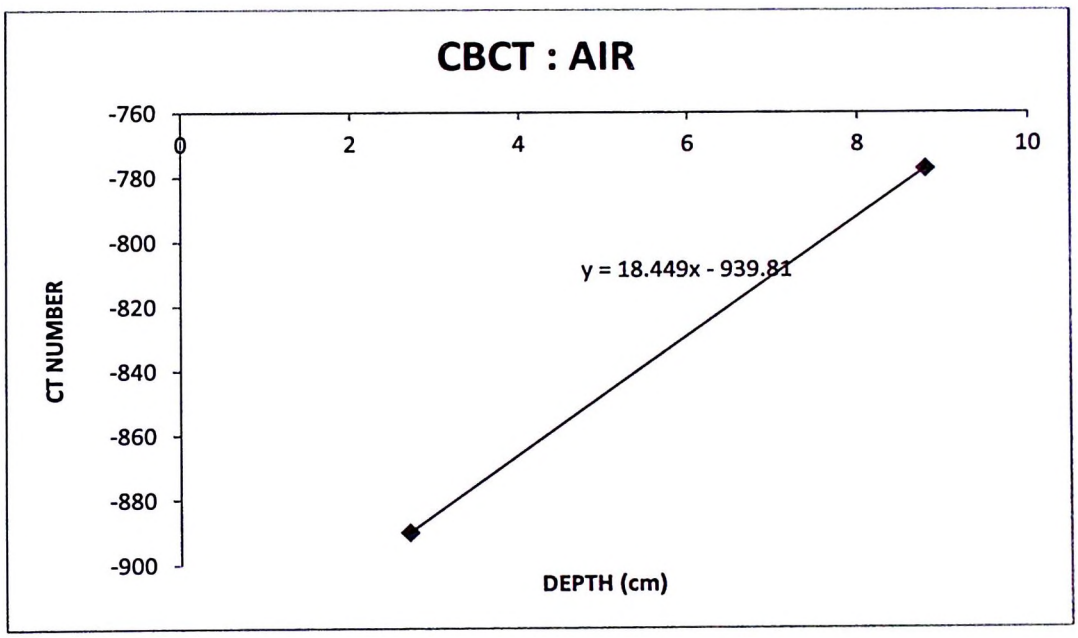

Figure 4.1: Graph of CT number against depth for air using CBCT modality.

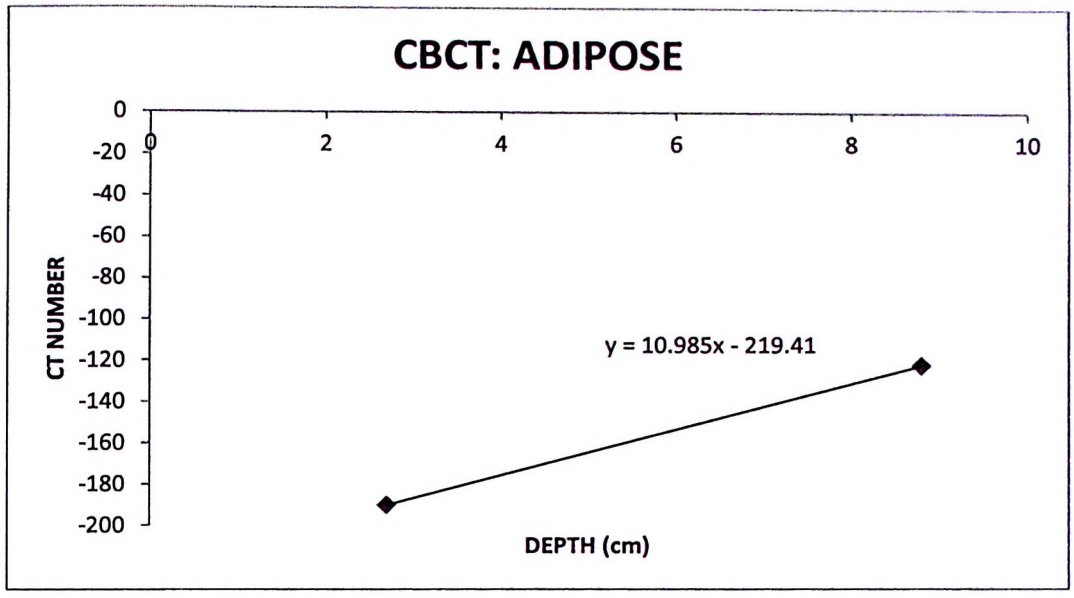

Figure 4.2: Graph of CT number against depth for adipose using CBCT modality.

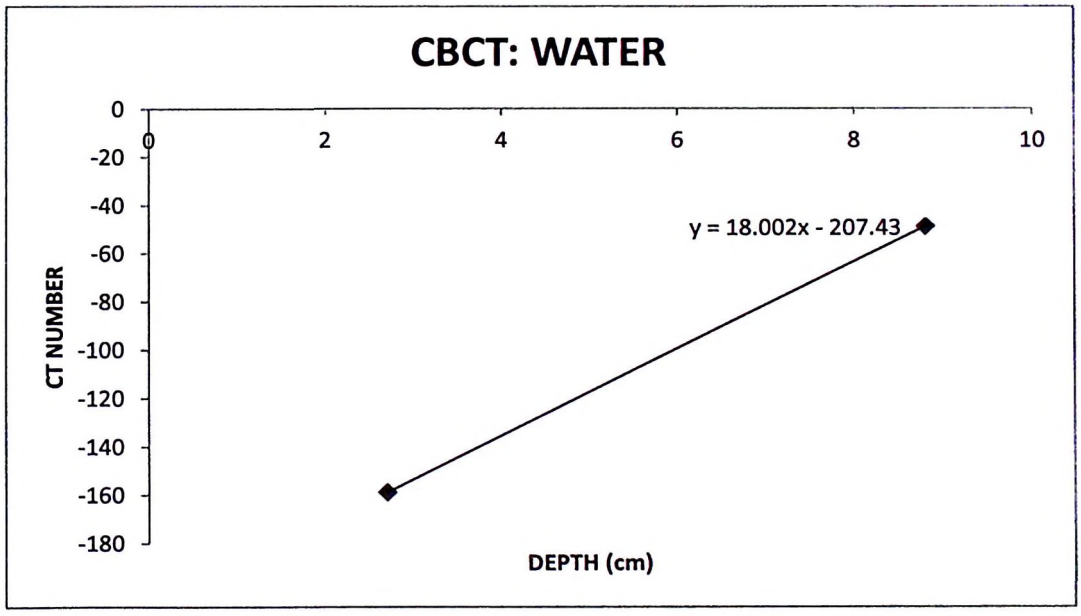

Figure 4.3: Graph of CT number against depth for water using CBCT modality.

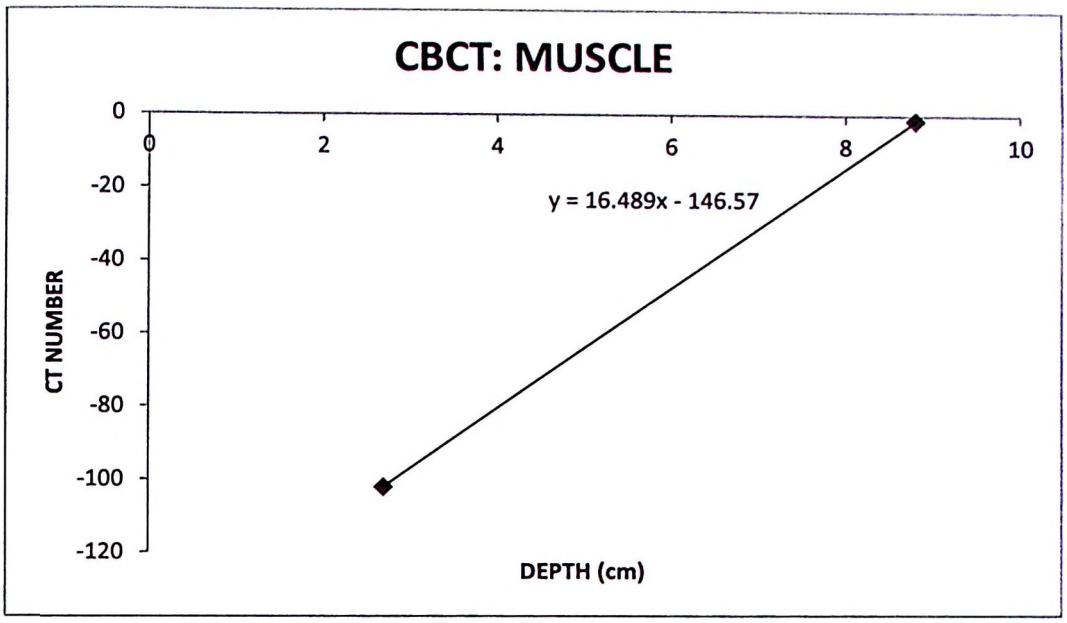

Figure 4.4: Graph of CT number against depth for muscle using CBCT modality.

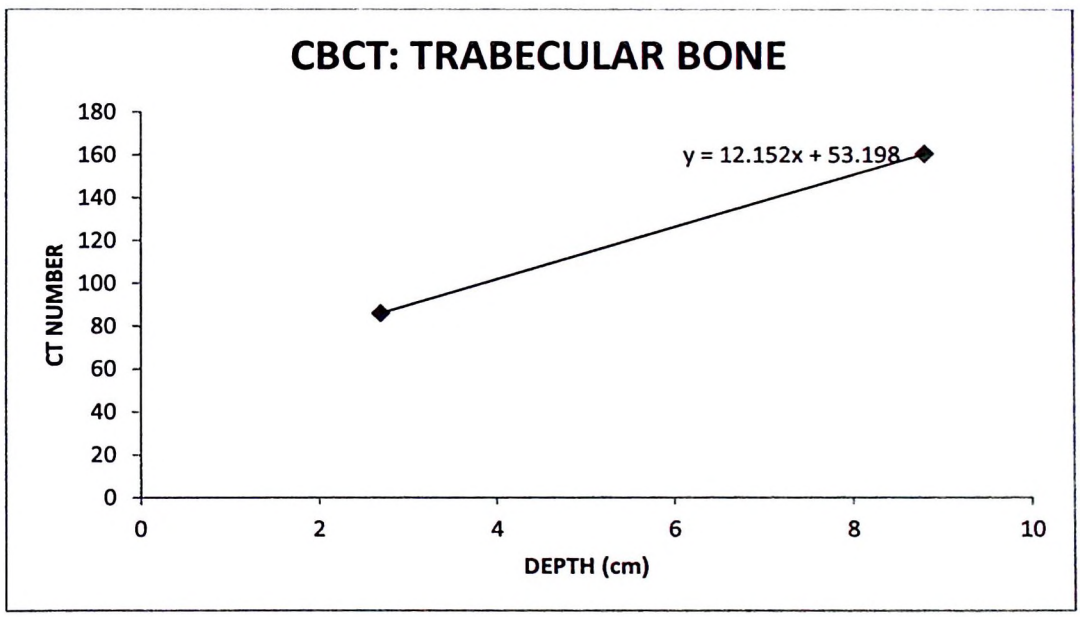

Figure 4.5: Graph of CT number against depth for trabecular bone using CBCT modality.

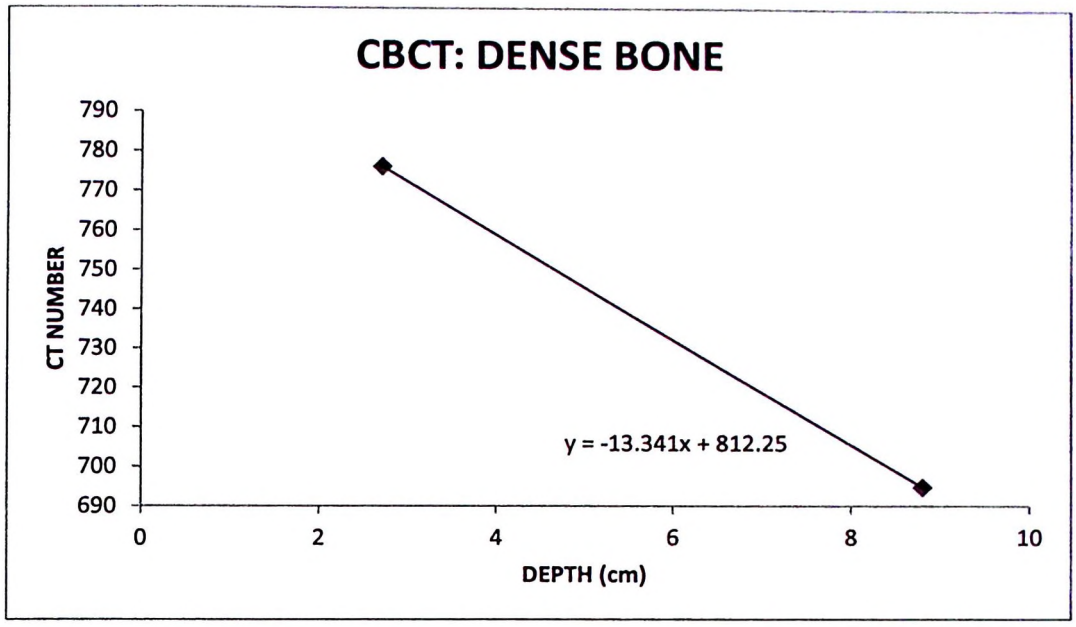

Figure 4.6: Graph of CT number against depth for dense bone using CBCT modality.

The CT number shows significant increment as the depth from electron density phantom increased. As illustrated in the figures, the increased of CT number occurs in most tissue densities represented by tissue equivalent plug phantoms. However, the dense bone plug phantom having physical density 1.53 g/cm^3, shows decreasing pattern of CT number at increased depth. Most of the material shows linearity of increased CT number at increased depth depicted by the gradient range between 10.9 and 18.5. The air cavity having mass density of 0 g/cm^3 showed the highest rate of increased CT number at increased depth while the lowest rate of increased CT number at increased depth was shown by adipose tissue equivalent (physical density : 0.96 g/cm^3).

The table of percentage difference between CT numbers at depth for each tissue equivalent plug phantoms is presented in Table 4.1. The highest percentage difference value is muscle with 6842.18%. This shows dramatic decrease of CT

number at central part than peripheral part of the electron density phantom which are -1.47 HU and -102.05 HU respectively. The dense bone plug phantom gave the lowest percentage difference value with 11.72% with the CT number value of 694.85 HU and 776.23 HU at central and peripheral part of the electron density phantom respectively.

Table 4.1: Average percentage difference of CT number at between central and peripheral position in electron density phantom for CBCT image.

Type of material/ tissue equivalent	Average percentage difference between depths (%)
Air	-14.475
Adipose	-54.595
Water	-224.011
Muscle	-6842.177
Trabecular bone	46.291
Dense bone	-11.716

4.1.2 CT number at different depths on CT Images.

The graph of CT number against depth from surface of electron density phantom for various tissue equivalent plug phantoms on CT image were illustrated in Figure 4.7 until 4.16. Interpolation lines were drawn between the points of measurement to determine the rate of change of CT numbers at increased depth.

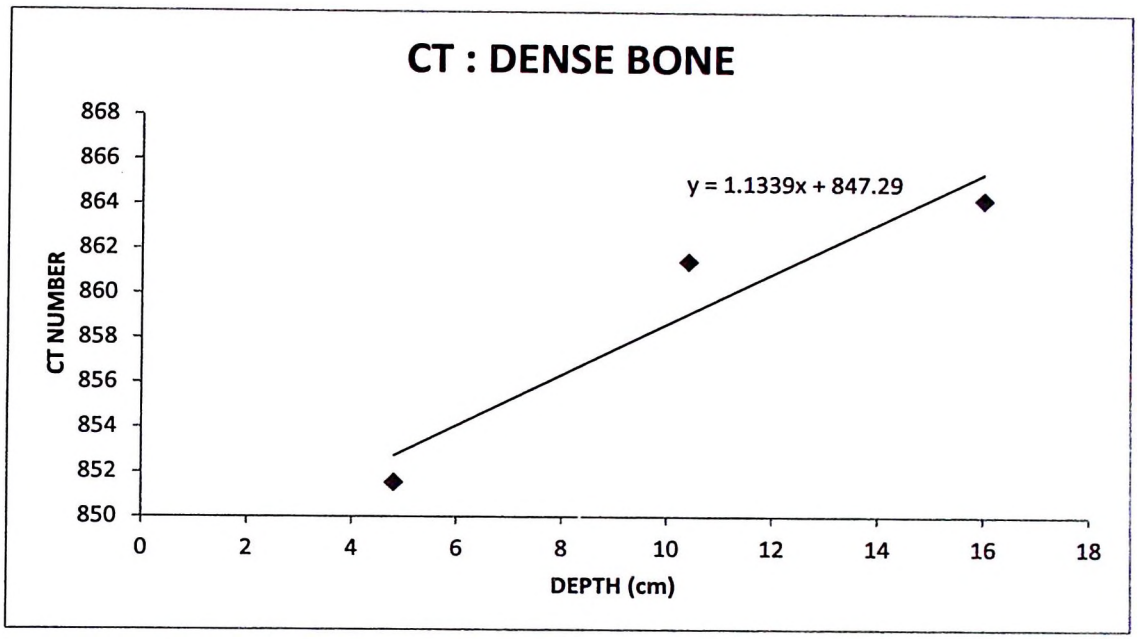

Figure 4.7: Graph of CT number against depth for dense bone tissue equivalent using CT modality.

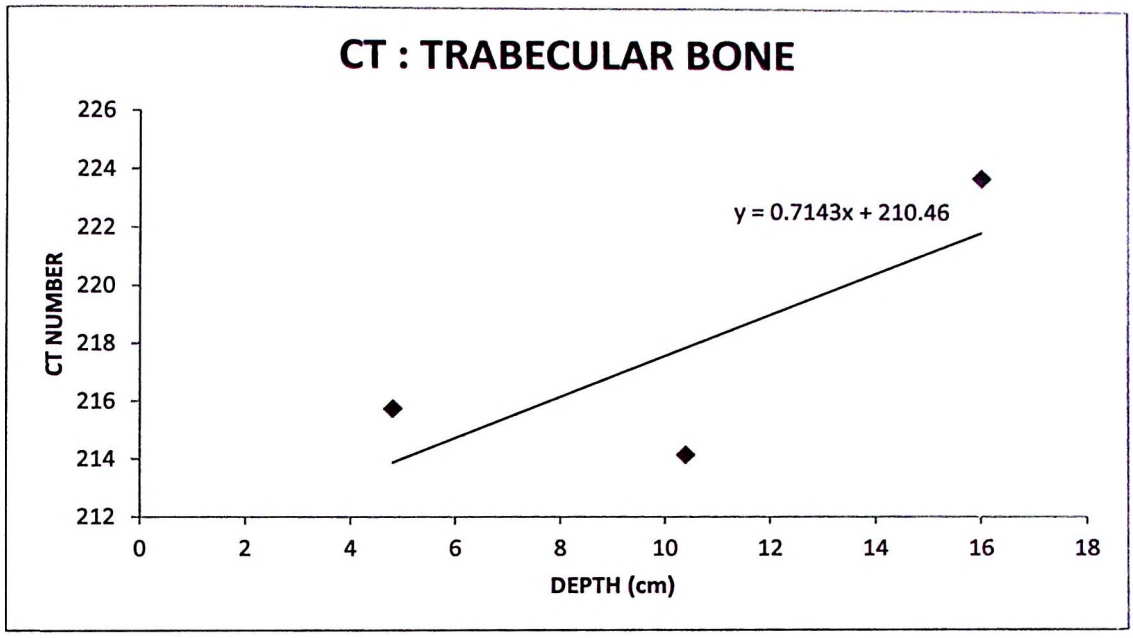

Figure 4.8: Graph of CT number against depth for trabecular bone tissue equivalent using CT modality.

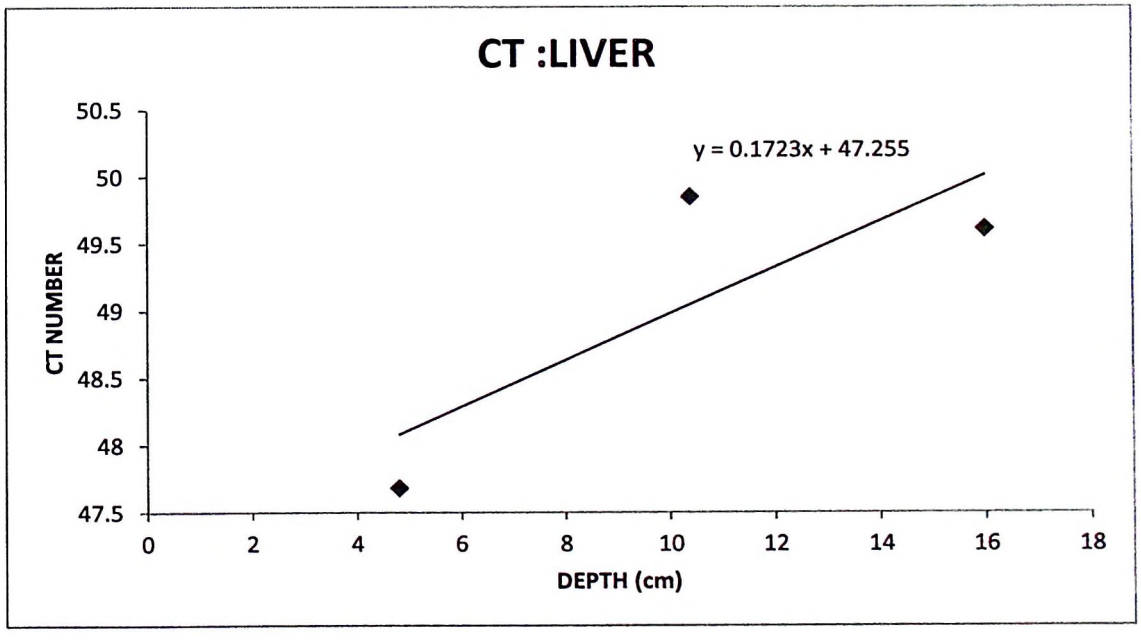

Figure 4.9: Graph of CT number against depth for liver tissue equivalent using CT modality.

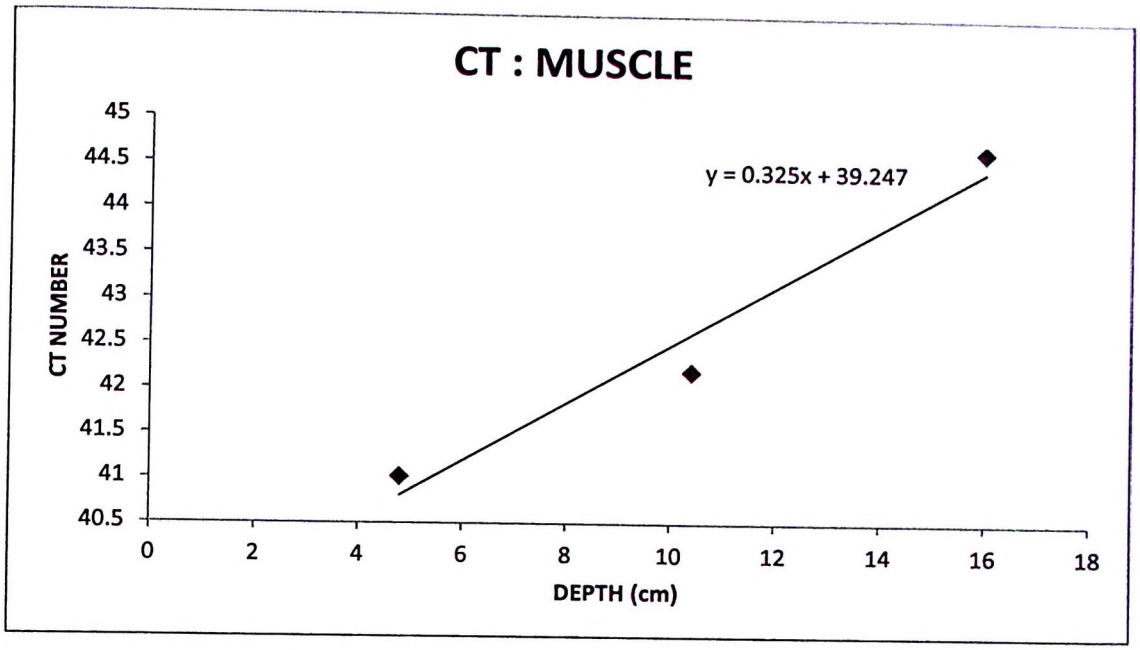

Figure 4.10: Graph of CT number against depth for muscle tissue equivalent using CT modality.

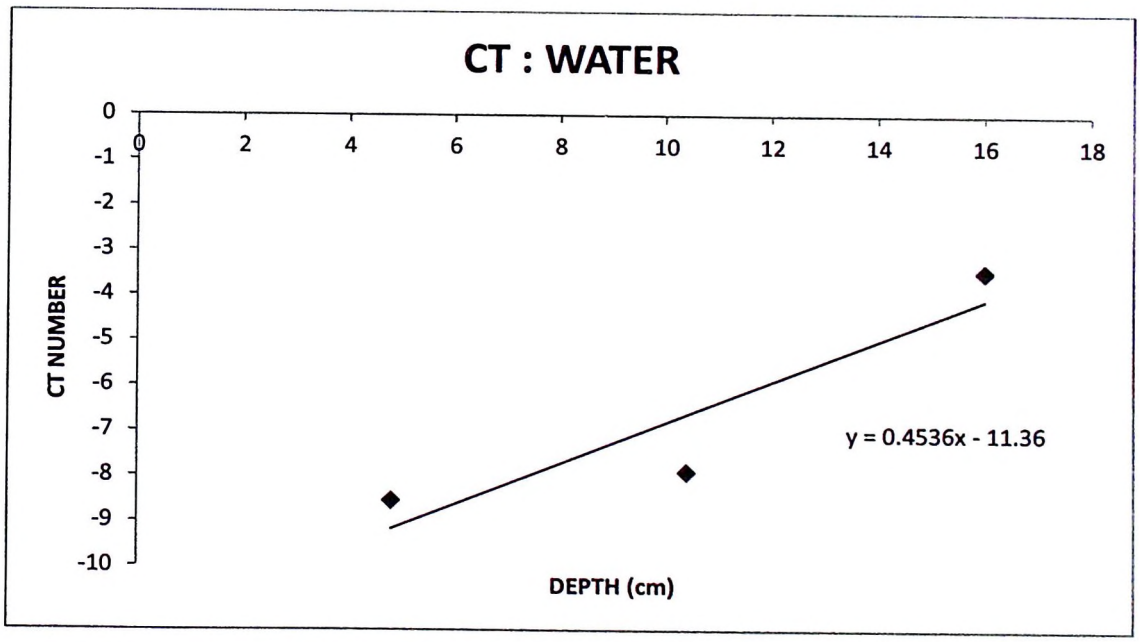

Figure 4.11: Graph of CT number against depth for water using CT modality.

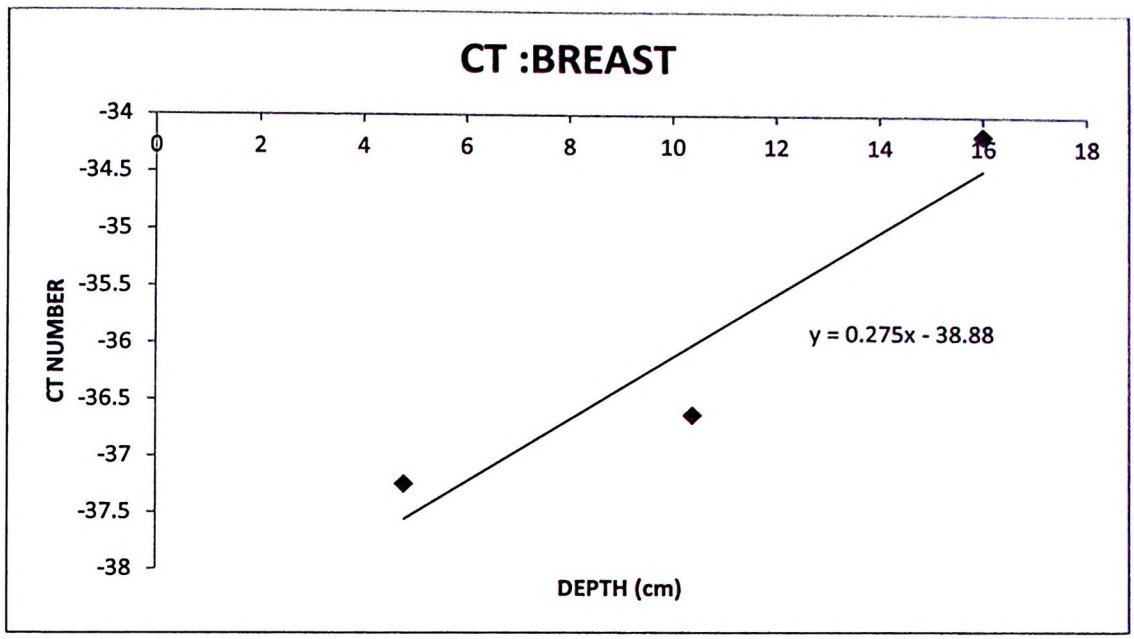

Figure 4.12: Graph of CT number against depth for breast tissue equivalent using CT modality.

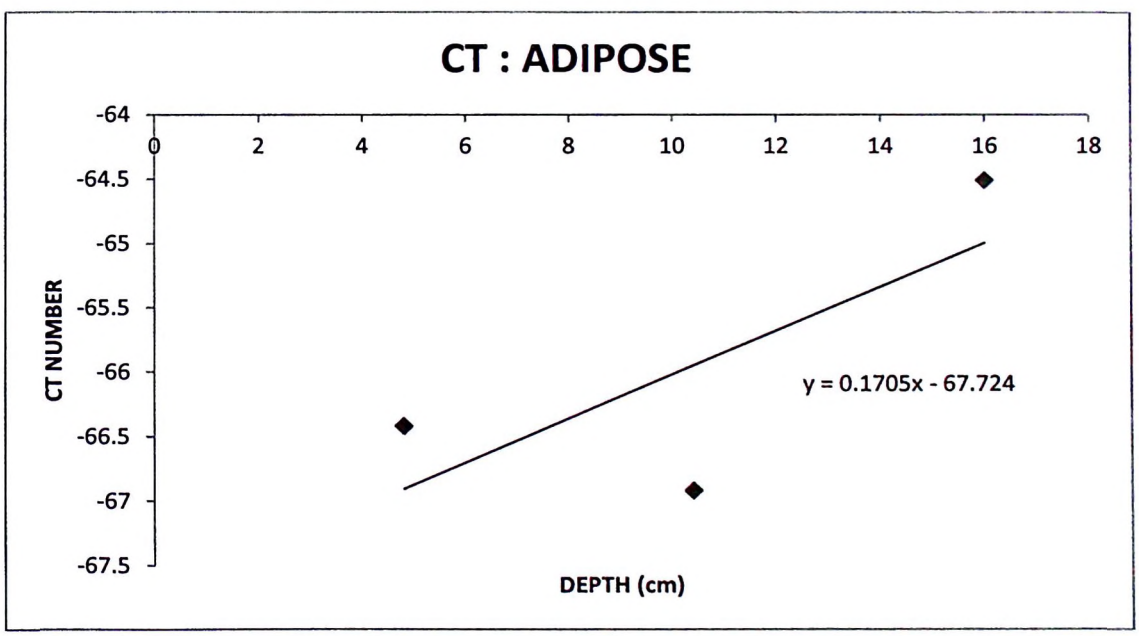

Figure 4.13: Graph of CT number against depth for adipose tissue equivalent using CT modality.